https://doi.org/10.32604/zkg.2024.06.01

Hydration and mechanical properties of less clinker cement incorporating chemical admixtures

Lili Wu, Congxi Tao*, Zhuoguang, Teng, Kunfu He, Jing Zhou, Shiguang, and Rong Peng
*China Resources Cement Technology Research and Development (Guangxi) Company Limited, Nanning, Guangxi/China

ABSTRACT: This study intended to enhance the mechanical properties of cement with less clinker content through the addition of composite admixtures (JT-GA), and decreasing the amount of CO2 released in cement production. In this investigation, the effects of incorporating JT-GA on the grinding efficiency, setting time, standard water demand, mechanical properties, hydration heat, and hydrates of cement samples, P80-1-0 (80% clinker, H19-GA), P74-1-0 (74% clinker, 0.05% H19-GA), and P74-1-1 (74% clinker, 0.05% H19-GA and 0.1% JT-GA), were examined. Results indicated that the mechanical properties of cement with less clinker (P74-1-1) were significantly improved through the addition of JT-GA. Compared to cement with 80% clinker content (P80-1-0), the compressive strengths at 3 d and 28 d were increased by 6.5% and 11.3%, respectively. This improvement was attributed to the use of JT-GA, which leads to a more uniform particle size distribution in cement with reduced clinker content and significantly promoted the dissolution of Fe^{3+} and Al^{3+} ions from ferric phases to react with aluminates, thus facilitating the formation of Hc/Mc, leading to the stabilization of ettringite. This further reduced porosity and increased the compressive strength. Additionally, the incorporation of JT-GA had minimal impact on the setting time and water demand for normal consistency of cement with reduced clinker content.

1 Introduction

Cement is the most extensively used binding material in plain concrete and reinforced concrete applications [1]. In 2023, China's cement production fell by 13.91% compared to the 2.35 billion t produced in 2019, but it still accounted for half of the global output, remaining a considerable figure. Consequently, a significant amount of CO_2 and waste gas is constantly being released into the environment. Long-term research and practice have demonstrated that the utilization of supplementary cementitious materials (SCM) to replace a portion of clinker in cement can achieve cost savings, enhance cement performance, facilitate the reuse of solid waste, and reduce carbon dioxide emissions [2]. Therefore, the research on maximizing the use of SCM in place of clinker, without compromising the mechanical properties and working performance of cement, has garnered widespread attention for the purposes of cement decarbonisation and sustainable development.

Limestone (LS) is widely distributed on earth and inexpensive, making it a widely studied and used SCMs material. The main interaction of LS in ternary blend, which can act as both a filler and an active reactant, has been extensively studied. As a filler, LS powder increases the effective water available for hydration and consequently space [3] for hydration grow. LS has been reported that it can impart a plasticizing effect in fresh Portland cement paste, physically improve the denseness of hardened Portland cement paste due to the filling effect and slightly increased early strength in optimum use [4–6]. Menendez et al. [7] studied the effect of replacing cement with LS (up to 20%) and granulated blast-furnace slag (BFS, up to 30%) on mechanical properties. Results show that the ternary blended cements (about 5–15% LF and 0–20% BFS) offer mechanical, economic and environmental advantage over the binary blended cements and plain Portland cements. the contribution of LF to hydration degree of Portland cement at 1 and 3 d increases the early strength of blended cements containing about 5–15% LF and 0–20% BFS. Because LS filler contributes to the early strength and the blast-furnace slag increases the long-term strength by the cementing reaction that refines the pore systems. As an active reactant, LS provides nucleation sites during hydration [8]. Besides, the calcite present in LS can react with the aluminate phase to form hemicarbonate (Hc) and monocarbonate (Mc) promotes the dissolution of Fe^{3+} and Al^{3+} ions from ferric phases to react with aluminates, thereby facilitating the formation of Hc/Mc phases, which prevents the transformation from ettringite (AFt) to monosulfoaluminate (AFm) [9]. Weerdt [10] investigated the interaction between LS powder and fly ash in ternary composite cement. Results showed pozzolanic reaction of fly ash

PROCESS

brought additional aluminates, which amplify the interaction of LS powder with the AFm and AFt hydration phases, leading to the formation of carboaluminates at the expense of monosulphate and thereby stabilizing the ettringite. This synergistic effect between LS powder and fly ash improved mechanical properties that persist over time. Adu-Amankwah [11] studied the hydration kinetics, microstructure and pore solution composition of ternary slag-LS cement. The author found that the presence of LS enhanced both clinker and slag hydration. The nucleation effects account for enhanced clinker hydration while the space available for hydrate growth plus the lowering of the aluminium concentration in the pore solution led to the improved slag hydration. Therefore, exploring ternary cement blends that utilize can overcome the disadvantages associated with the separate use of LS and Al-rich SCM. A comprehensive study of ternary cement, and even multicomponent cement, leveraging local waste solids in combination with LS, holds significant potential for reducing clinker usage and CO_2 emissions.

As a common grinding aid in cement mills, alkanolamine can significantly reduce the energy consumption and enhance cement properties [12]. Wang et al. [13] summarized that triisopropanolamine (TIPA) has the ability to hasten the dissolution of Fe^{3+} and Al^{3+} ions present in C4AF, and it aids in the formation of ettringite by promoting the creation of the compound TIPA-Fe. Consequently, this process enhances the dissolution of the ferrite phase, which in turn facilitates the dissolution of other phases. Consequently, the induction period is shortened, and the overall silicate reaction is somewhat accelerated, leading to improved mechanical properties at the early stage. Shi et al. [14] conducted an investigation into the impact of TIPA on the strength, hydration process, and microstructure of LS Portland cement. The findings revealed that the mechanical strength of LS Portland cement was bolstered by the addition of TIPA. Specifically, when 0.02%, 0.05%, and 0.08% TIPA were incorporated, the 7 days strength increased by 6.3%~12.7%, while the 28 days strength also exhibited an upward trend of 4.7%~12.3%. The authors attributed this enhancement to the improvement in the microstructure of the LS Portland cement paste brought about by TIPA. Shi et al. [15] investigated the interactive impact of TIPA, NaCl, and LS on compressive strength and hydration. The findings revealed that the combination of TIPA and NaCl could enhance both the early and later age compressive strength of Portland cement mortars as well as Portland cement- LS mortars. No significant interactive effects on the improvement of strength were noticed among these three additives. Nevertheless, the isothermal calorimetry results demonstrated a clear interaction between TIPA and NaCl. It was discovered that NaCl augmented the effectiveness of TIPA by facilitating two transitions: the conversion of AFt to AFm in the Portland cement sample, and the conversion of carboalumiante phases in the Portland-LS cement sample. To some extent, studies have found that the strength-enhancing mechanism of DEIPA and EDIPA is probably similar to TIPA. Ma et al. [16] observed that DEIPA facilitates the formation of AFt and boosts the second hydration rate of aluminate and ferrite phases. Additionally, it triggers the conversion of AFt into AFm and the creation of microcrystalline portlandite (CH) during the early stages. Furthermore, DEIPA speeds up the hydration process of alite, leading to a reduction in pore size and porosity. Lu et al. [17] studied the effect of EDIPA dosage on the hydration process and strength augmentation of Portland cement. The findings revealed that EDIPA inhibits the formation of AFt, slows down the dissolution of gypsum, and speeds up the hydration rate of both the aluminate and ferrite phase, along with the transformation of AFt to AFm. Furthermore, EDIPA also facilitates the hydration of alite and the formation of CH, resulting in a significant enhancement of mechanical properties After 28 d. However, the impact of concurrently applying compound active additives to composite limestone-cement on its mechanical properties remains unexplored.

The primary objective of this research is to enhance the mechanical properties of a limestonecement based composite system with reduced clinker content by incorporating a chemical compound enhancer, JT-GA. In this study, mortars and pastes were prepared using a composite limestonecement with a 6% reduction in clinker content and a JT-GA dosage of 0.1% by weight of the powder materials. The mechanical strength was measured up to 28 days. In order to clarify the underlying mechanism, the hydration heat, hydration products and microstructure of hardened pastes was investigated in terms of Isothermal calorimetry, XRD, TG-DTG and MIP. The experimental results were expected to provide guidance on the utilization of chemical composite enhancer in less clinker limestone-cement based composite material.

2 Experiment

2.1 Materials

Raw materials for cementitious systems: clinker, gypsum, and blended materials, sourced locally from CR BLDG Materials Tech. Two composite admixtures were used. One is H19-GA, a grinding aid commonly used by the cement factory for cement production at a dosage of 0.05 wt.% of total mass of cement. The other is a newly developed compound strength enhancer (JT-GA), dosed at 0.1 wt% of total mass of cement. The phase composition of raw materials for cementitious materials was examined by XRD and the result is shown in Figure 1.

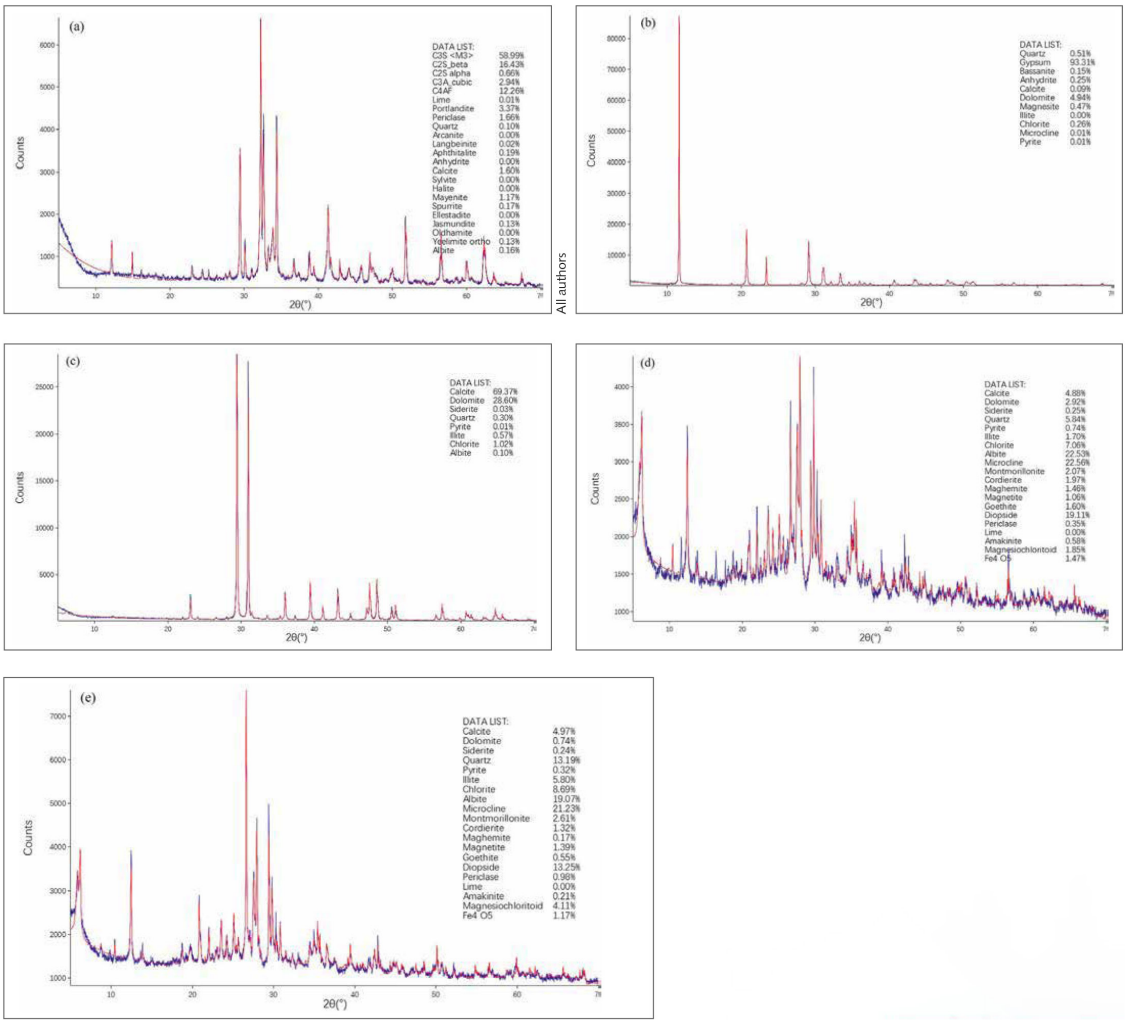

All authors

1 **XRD patterns of raw materials for cementitious materials: (a) clinker, (b) Gypsum, (c) limestone, (d) slag and (e) coal ash**

2.2 Cement grinding process

To validate the effects of JT-GA on grinding and strengthening, cement and less clinker cement grinding operations for this study were performed in a Type SM-500 laboratory ball mill. The inference sample included 4 kg of clinker, 0.2 kg of gypsum, 0.8 kg of blended materials. The second and third sets separately comprised 3.7 kg of clinker, 0.2 kg of gypsum, 1.1 kg of blended materials. The detailed material ratios and dosage of grinding aids are presented in Table 1. The main chemical composition of the three cement samples is presented in Table 2.

Table 1 **Materials ratio of the three cement samples and dosage of grinding aids**

Sample	Clinker	Gypsum	Limestone	Coal ash	Slag	H19-GA	JT-GA
	kg	kg	kg	kg	kg	g	g
P80-1-0	4.0	0.2	0.5	0.15	0.15	2.5	-
P74-1-0	3.7	0.2	0.6	0.25	0.25	2.5	-
P74-1-1	3.7	0.2	0.6	0.25	0.25	2.5	5

Table 2 **Chemical composition of the three cement samples [%]**

Sample	SiO_2	Al_2O_3	Fe_2O_3	CaO	MgO	SO_3	K_2O	Na_2O	LOI
P80-1-0	20.15	5.43	11.48	57.48	2.21	3.01	0.70	0.23	6.55
P74-1-0	20.87	5.79	3.78	55.21	2.34	2.88	0.79	0.32	7.55
P74-1-1	22.72	6.21	3.96	55.10	2.44	3.15	0.85	0.36	4.36

2.3 Characterization of cement

2.3.1 Blaine surface area and sieve residue value of cement

The Blaine surface area of cement was determined according to the standard method of GB/T 8074-2008. The sieve residue value of cement was performed based on the Chinese national standard GB/T 1345-2005.

2.3.2 Physical and mechanical properties: Characterization of the produced cement

The standard water requirement and setting time tests were conducted based on the Chinese national standard GB/T 1346-2011. All mortar samples were prepared in accordance with Chinese national standard GB/T 17671-2021 and molded with a size of 40 × 40 × 160 mm^3, three samples of each group. The flexural strength of the specimens was tested by DKZ-5000, Wuxi Jianyi Instrument & Machinery Co., Ltd, while the compressive strength was evaluated at a loading rate of 2.4 KN/s by YAW-300B, Jing Yuan Machinery.

2.3.3 Isothermal calorimetry

The W/B ratio (by weight) of cement was 0.5. The tests of the three cements were measured by an isothermal conduction calorimeter with TAM Air by TA instruments and conducted over a 28 d period. The experimental temperature during the test was 20 °C.

2.3.4 X-ray powder diffraction

All paste samples were molded with a size of 10 × 10 × 10 mm^3, which were cured for one day in a > 98% R.H. and 20±1 °C chamber. After that, these samples were placed into water (20 °C) for continued curing and the hydration was stopped until 3 d, 14 d and 28 d by submerging small pieces in alcohol. The pieces were then dried at 45 °C for 24 h and pulverized for XRD and TG experiments. The phase composition of different cement pastes was characterized by Bruker S8 Tiger X. The sample was scanned from 5°~70° with the scanning speed 0.4 second per step.

2.3.5 Thermogravimetric analysis

Thermogravimetric analysis(TG) of different cement pastes were performed on NETZSCH STA 449F3 and the test temperature was 25~1000 °C. The heating rate was 10 °C/min during the experiment.

2.3.6 Mercury intrusion porosimetry analysis

The mercury intrusion porometers (MIP) was tested on AutoPore IV 9500 by Micromeritics Instrument Corporation. The size of samples is 3-5 mm. To maintain consistency in the data source, the MIP samples were derived from the mortar particles crushed from the specimens utilized for strength testing. The range of the pore diameter measured in this study is 5~360,000 nm.

3 Results and discussion

3.1 Evaluation of grinding efficiency

The specific surface and sieve residue values of three cement sets are shown in the Figure 2. It shows that the Blaine surface area of less clinker sample with the same grinding aid (P74-1-0) apparently increased 20 m^2/kg and the 45 µm sieve residue value slightly increased by 0.8% in comparison with control sample (P80-1-0). This result was attributed to increasing substitutions of clinker by blends with lower Mohs hardness in the same grinding duration. When additionally adding the JT-GA, the opposite trend was presented, in which the less clinker sample with two grinding aids (P74-1-1) had 5 m^2/kg lower Blaine surface area and 2.1% smaller 45 µm sieve residue values than that of P80-1-0. It suggested that the JT-GA may have facilitated a more uniform particle size distribution with fewer fines by promoting the breakage of larger particles into smaller ones, which led to much lower 45 µm sieve residue value. A slightly decrease in Blaine surface area also indicated a reduction in the fine particle fraction [18].

3.2 Setting time and standard water requirement

From Figure 3(a), it can be observed that P74-1-0 leads to an extension in the final setting time from 226 min to 231 min in comparison with P80-1-0. This was attributed to the decrease in the number of hydration products, which subsequently delays the final setting process. Comparatively, when in presence of JT-GA, the initial setting time of

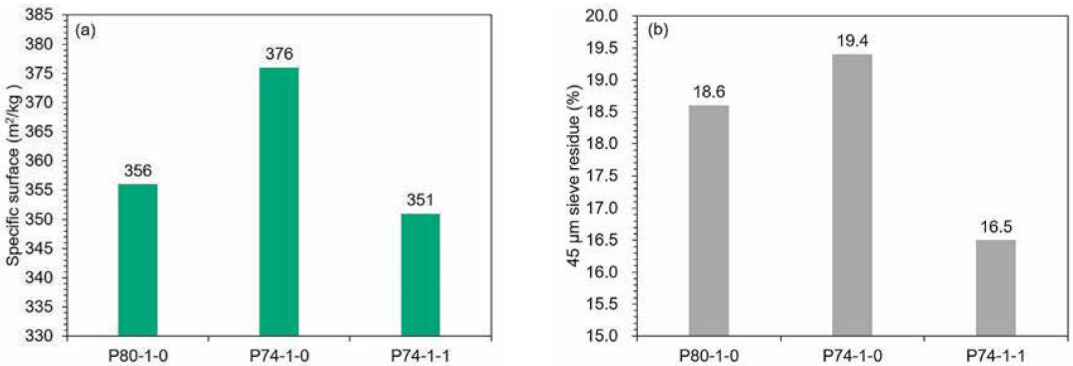

2 (a) Specific surface and (b) sieve residue value of the three cement samples

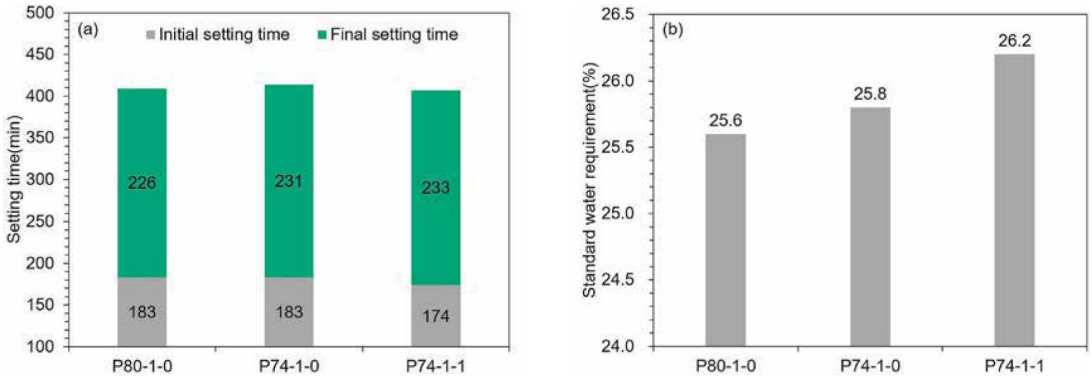

3 (a) Setting time and (b) standard water requirement of the three cement samples

P74- 1-1 was shortened to 174 min in comparison with P80-1-0. This was attributed to the combined the effect of the chemical and grinding aid effects of JT-GA, which led to a higher degree of hydration and a shortened setting process.

Additionally, as shown in Figure 3(b), reducing the amount of clinker resulted in an increase in standard water requirement, with a 0.2% increase without adding JT-GA and a 0.6% increase with the addition of JT-GA, respectively. This may be attributed to the finer grinding of the cement based on the above analysis, which increased the specific surface area and decreased the sieve residue value thus required more water to wet the surface. Furthermore, finer cement particles exhibited higher chemical activity, leading to increased reaction rates and degrees with water, consequently necessitating more water for the reaction.

3.3 Mechanical properties of the cement pastes

As can be seen from Figure 4(a), the compressive strength of the P74-1-0 sample was sharply lower than that of the P80-1-0 sample, which reduced by 18.2% and 12.3% at 3 d and 28 d, respectively. This was mainly because the addition of blends reduced the amount of clinker, which was the major contribution to the mortar strength, despite the certain beneficial caused by the higher specific area. This result indicated that high content of blends had a great adverse effect on the mechanical strength of mortar and this should be carefully considered in the utilization of blends.

When incorporated with JT-GA, the mechanical strength of the less clinker sample(P74 1-1) was obviously improved. From the experimental results, it was clear that the addition of 0.1% JT-GA increased the 3 d and 28 d compressive strength of the less clinker sample by 6.5% and 11.3% in comparison with P80-1-0 sample, respectively. The results implied that JT-GA has a positive effect on the development of mechanical strength. The presence of JT-GA has facilitated a more uniform particle size distribution, which highly improved the hydration reaction. Meanwhile, JT-GA is a mixture that can enhance the hydration process of the less clinker sample by complexing with C4AF. Its potential effects seem promising compared to TIPA, which promotes the dissolution of ferric phases to react with aluminates, leading to the formation of Hc and Mc. The variation pattern of flexural strength (see Figure 4(b)) was consistent with that of compressive strength.

3.4 Hydration heat

The hydration process of cement can be effectively reflected through the measurement of hydration heat. In order to further investigate the effect of JTGA on the hydration process of the less clinker content cement system, the hydration heat evolution rate and the cumulative hydration heat of cement pastes were performed, which is shown in Figure 5.

In Figure 5(a), upon initial contact between cement and water, dissolution occured immediately,

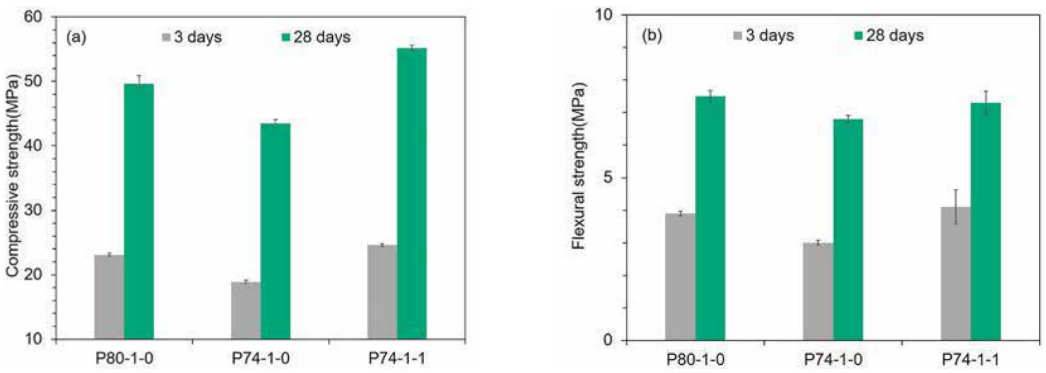

4 (a) Compressive strength and (b) flexural strength of the three cement mortars

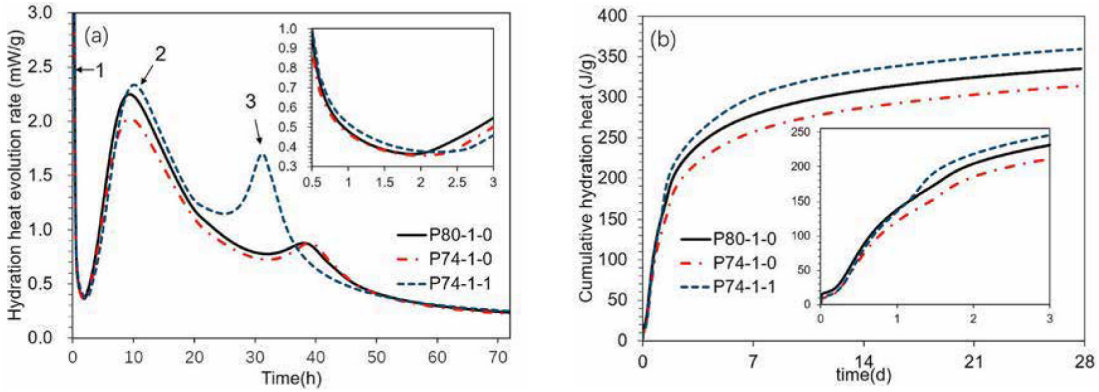

5 (a) Hydration heat evolution rate and (b) cumulative hydration heat of the three cement pastes

releasing a significant amount of heat, represented by peak 1. However, due to the brevity of this exothermic peak, accurate data for analysis is challenging to obtain [13]. Subsequently, it was the induction period, during which the P80-1-0 sample exhibited a higher hydration exothermic rate compared to the P74-1-0 sample. This was attributed to the reduced amount of clinker, which led to decreased dissolution heat release and slower nucleation of C-S-H, thus prolonging the time to reach the acceleration period. The addition of JTGA to P74-1-1 resulted in an improved hydration exothermic rate within the first two hours, indicating an increase in the dissolution of cement with reduced clinker content. Simultaneously, it significantly extended the cement induction period. The second peak (peak 2) was typically attributed to the exothermic reaction resulting from rapid alite hydration [19]. Although P74-1-0 extended the induction period, the position of its second exothermic peak was relatively consistent, differing only by 0.05 h, with a peak value that was 10.03% lower than P80-1-0. In contrast, P74-1-1 with added JT-GA exhibited a delayed peak position by 0.67 h compared to P80-1-0, and a peak value that was increased by 15.45%. This suggested that JTGA enhances the hydration of C3S in the reduced clinker system, as reported in other literature [20-21].

Approximately 26.7 h later, a third exothermic peak (peak 3) emerged, believed to be the result of the conversion of AFt to AFm [22]. The positions of the peak 3 for P80-1-0, P74-1-0, and P74-1-1 were 38.10 h, 39.05 h, and 31.18 h, respectively, with peak values of 0.88 mW/g, 0.88 mW/g, and 1.70 mW/g. Compared with the other two samples, P74-1-1 exhibited an earlier peak position by 6.91- 7.86 h and a peak height increase of 93.85%. As mentioned above, calcites reacted with aluminates to form calcium aluminates, and the reaction rate was faster than that of AFt to AFm conversion, and thus inhibiting this process. In this study, compared with the P80-1-0 sample, the P74-1-1 sample had an increased portion of calcite, finer powder and furthermore adding JT-GA, which substantially promoted the formation of calcium aluminates. Based on the above analysis, it can be inferred that the emergence and enhancement of the peak 3 was due to the acceleration of the formation reaction of calcium aluminates caused by the depletion of gypsum, rather than the conversion of AFt.

The cumulative hydration heat release curve is presented in Figure 5(b) and the cumulative hydration heat of samples are listed in Table 3. The cumulative heat of the P74-1-0 sample release at 3 d decreased from 230.96 to 211.06 J/g compared to the P80-1-0. However, upon the addition of JT-GA, it increased to 245.48 J/g. At 28 d, the difference in cumulative heat release between the cement system with JT-GA and the P80-1-0 further increased, from a difference of 14.52 J/g to 24.51 J/g. This suggested that the addition of JT-GA enhanced the hydration reaction during the extended cement curing period from 3 to 28 d.

Table 3 Cumulative heat release of the three cement pastes

Sample	Cumulative hydration heat [J/g]				
	12 h	24 h	48 h	3 d	28 d
P80-1-0	76.47	138.09	203.94	230.96	334.94
P74-1-0	64.31	121.16	185.00	211.06	313.83
P74-1-1	69.00	135.56	218.20	245.48	359.45

3.5 Hydrates analysis

3.5.1 Phase formation

In Figure 6, the XRD pattern of P80-1-0, P74-1-0 and P74-1-1 cured 3 d and 28 d were comparatively studied. As shown in Figure 6(a), in P80-1-0 sample, the peak of C3S, C2S, C4AF, AFt, Hc and Mc were seen clearly [13]. During the cement hydration process, calcite would react with calcium aluminate preferentially to form Hc (10.8° 2θ) and Mc (11.7° 2θ) After the gypsum was completely consumed in the presence of LS, and the transformation of AFt to AFm was hindered. Compared to the P80-1-0 sample, the P74-1-0 sample featured a 6 wt.% reduction in clinker usage and employed the same grinding aid. Although its XRD pattern remained similar to that of the previous sample, no Mc peak was observed. When 0.1% JT-GA was additionally incorporated, the intensity of peak of Hc/Mc increased significantly, indicating that JTGA promoted the formation of Hc and Mc in the

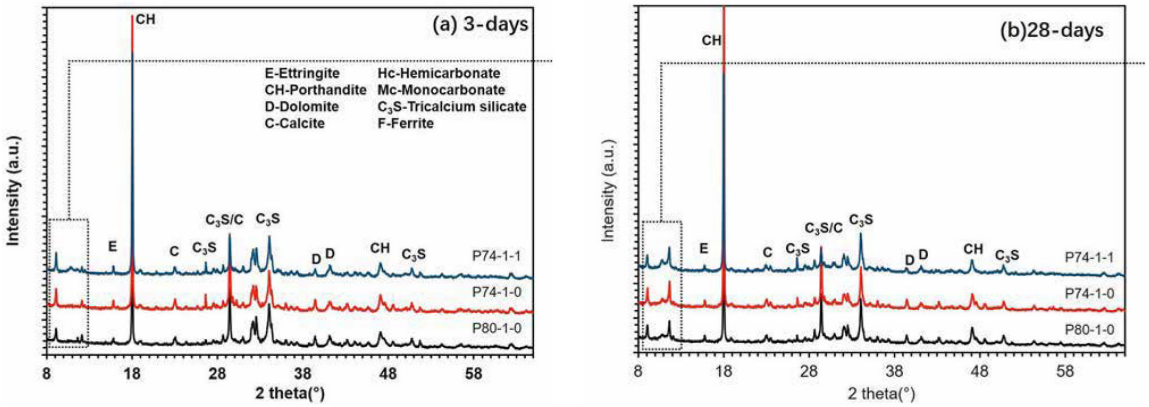

6 XRD patterns of the three cement pastes at (a) 3 d and (b) 28 d

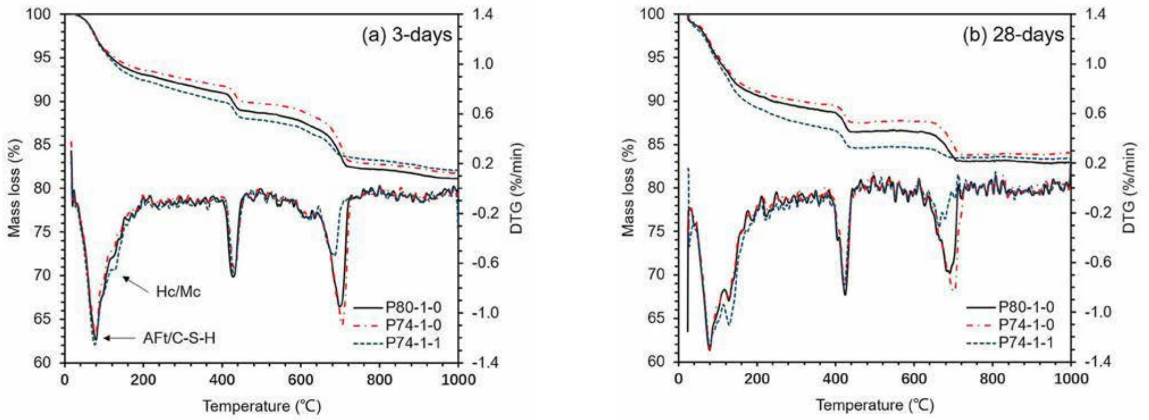

7 TG-DTG patterns of the three cement paste at (a) 3 d and (b) 28 d

less clinker system (P74-1-1). As shown in Figure 6(b), the increased Hc and Mc peaks in these three samples were seen obviously indicating the reaction between Hc with calcite to form Mc at 28 d. The near absence of the C4AF diffraction peak in the P74-1-1 sample indicated that JT-GA promotes the dissolution of Fe^{3+} and Al^{3+} ions from ferric phases to react with aluminates, thereby facilitating the formation of Hc/Mc.

3.5.2 TG-DTG analysis

The TG-DTG analysis of cement pastes containing P80-1-0, P74-1-0 and P74-1-1 are presented in Figure 7. As a previous study reported, the mass loss around 100 °C was caused by the dehydration of AFt or C-S-H and the mass loss around 150 °C was mainly ascribed to the decomposition of Hc or Mc [23-24]. In Figure 7(a), an obvious endothermic peak of Hc/Mc appeared in P74-1-1- contained paste implied the formation of Hc and Mc, while was undetectable in P74-1-0. At 28 d (see Figure 7(b)), the endothermic peak of Hc/Mc showed in all of the three cement samples and the Hc/Mc peak of Sample P74-1-1 was the most prominent. These trends were consistent with their XRD analysis results.

To quantitatively analyze the transformation of hydration products, mass loss of cement pastes in a different temperature range was calculated (see Table 4). The mass loss of P74-1-1 sample in the temperature range 50-200 °C was higher than that of sample P80-1-0 and P74-1-0 at all ages, which further verified the acceleration effect of JT-GA on less clinker cement system. The mass loss of sample P74-1-1 between 370-500 °C caused by the pyrolysis of potlandite showed 9.87% higher at 3 d and 8.96% higher at 28 d than that of sample P74-1-0. That was another key point verified the acceleration effect of JT-GA. Moreover, between 3 and 28 d, for all samples, contrary to the trend of increasing mass loss in the temperature range of 50-200 °C, the mass loss in the temperature ranges of 370-500 °C and 600-800 °C decreased significantly, indicating the continuous consumption and reaction of CH and calcite during the hydration process within this time period.

3.6 Pore structure

The pore structure of the three cement mortars was characterized with MIP, and porosity, pore diameter distribution ratio was obtained from

Table 4 Mass loss of the three cement pastes at different temperature range [wt.%]

Age	Sample	Temperature range [°C]				H	CH
		50~200 °C	370~500 °C		600~800 °C		
3-days	P80-1-0	6.33	2.54	5.56	8.87		10.44
	P74-1-0	5.77	2.23	6.17	8.00		9.17
	P74-1-1	6.94	2.40	3.70	9.34		9.87
28-days	P80-1-0	7.89	2.29	3.27	10.18		9.41
	P74-1-0	7.68	1.92	3.77	9.60		7.89
	P74-1-1	8.97	2.18	1.04	11.15		8.96

the results of MIP, as shown in Figure 8, Figure 9 and Table 5. As reported in the literature [25], pores in cement paste can be divided into four types: harmless pores (smaller than 20 nm), less harmful pores (between 20 and 50 nm), harmful pores (between 50 and 200 nm) and very harmful pores (bigger than 200 nm) [26-29]. Firstly, as shown in Figure 8, in all three samples, the porosity decreased significantly as hydration progressed, indicating that growth of hydrates filled the increasingly refining pores.

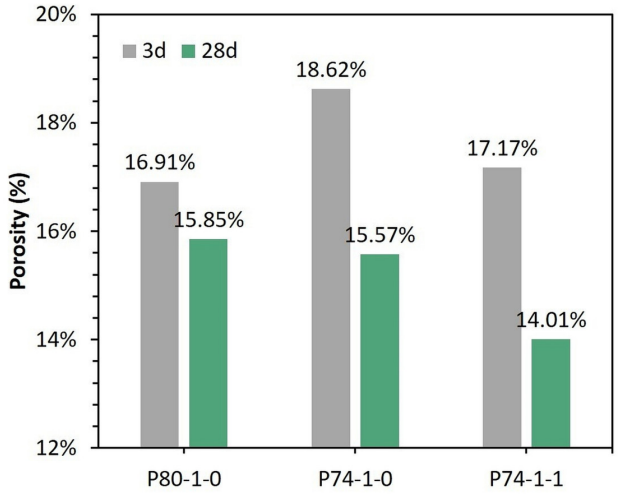

8 Porosities of the three cement mortars at 3 d and 28 d

Furthermore, at the age of 3 d (see Figure 9(a)), the porosity of the sample P74-1-0 was 1.71% larger than that of P80-1-0. After adding JT-GA, the porosity of the sample P74-1-1 was 17.17%, which was almost the same as that of P80-1-0 (16.91%). At the age of 28 d (see Figure 9(b)), the porosity of the three samples P80-1-0, P74-1-0 and P74-1-1 were 15.85%, 15.57% and 14.01% respectively. By adding JT-GA, the porosity of the sample P74-1-1 was made 1.84% lower than that of the samples P80-1-0, thus contributing to the strength.

It is noteworthy that, as shown in Table 5, at the age of 3 d, the increase in porosity of the lowclinker cement samples P74-1-0 and P74-1-1 was mainly attributed to pores with diameters below 50 nm. At the age of 28 d, regardless of whether additional additives were added, the porosities of P74-1-0 and P74-1-1 in pores with all diameters were lower than that of P80-1-0. This synergetic effect had previously been observed for ternary blends of Portland cement and limestone with fly ashes slags, and calcium aluminosilicate glasses [2]. For P74-1-0 and P74-1-1, contribution of more SCM material, $CaCO_3$ reacts with alumina species in the pore solution and forms calcium Hc and Mc phases, which were high-volume, spacefilling phases that reduce the porosity. This reaction stabilized ettringite formed by alumina and the available sulfate ions, reducing porosity further and increasing the compressive strength [30].

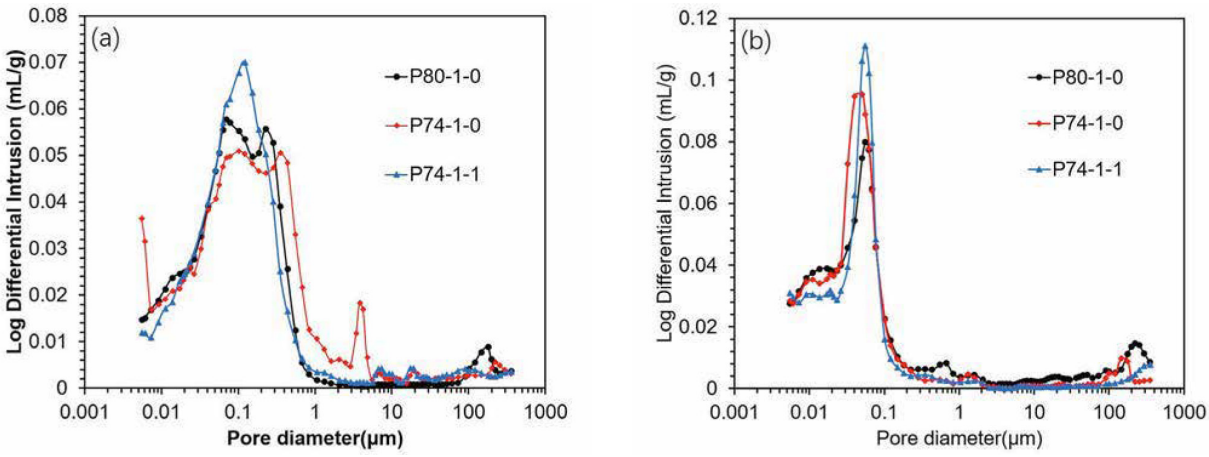

9 Pore size distribution of the three cement mortars at (a) 3 d and (b) 28 d

Table 5 **Pore structure of the three cement mortars at (a) 3 d and (b) 28 d**

Age	Series	Porosity [ml/g]	Pore diameter distribution ratio [ml/g]		
			~50 nm	50 nm-200 nm	200 nm~
3-days	P80-1-0	1.081	1.030	0.037	0.014
	P74-1-0	1.226	1.186	0.022	0.017
	P74-1-1	1.114	1.075	0.027	0.012
28-days	P80-1-0	1.170	1.066	0.055	0.049
	P74-1-0	1.111	1.063	0.038	0.010
	P74-1-1	1.041	1.000	0.016	0.026

4 Conclusions

(1) The Blaine surface area of the sample with less clinker (P74-1-0) apparently increased by 20 m^2/kg, and the 45 µm sieve residue value slightly increased by 0.8% in comparison with the control sample (P80-1-0). However, the addition of JT-GA showed a contrasting trend, as P74-1-1 had a 5 m2/kg lower Blaine surface area and 2.1% smaller 45 µm sieve residue values than P80-1-0. This indicated a more uniform particle size distribution with fewer fines

(2) P74-1-0 with less clinker led to a prolongation in the final setting time. However, with the addition of JT-GA, P74-1-1 had a shorter initial setting time. This result was consistent with the order of hydration heat release rates within two hours, as the rate of hydration affects the length of the setting time.

(3) The compressive strength of the less clinker sample (P74-1-0) was significantly decreased by 18.2% and 12.3% compared to P80-1-0 at 3 d and 28 d. With the addition of JT-GA, the compressive strength of P74-1-1 increased by 6.5% and 11.3% compared to P80-1-0 at 3 d and 28 d. The variation pattern of flexural strength was consistent with that of compressive strength.

(4) Through hydration heat, XRD, and TG-DTG examination, it was found that JT-GA promotes the dissolution of Fe^{3+} and Al^{3+} ions from ferric phases to react with aluminates, thereby facilitating the formation of Hc/Mc at all ages, leading to the stabilization of ettringite. Furthermore, TG-DTG showed that CH and $CaCO_3$ were constantly consumed and reacted.

(5) The MIP test results indicated that the porosity of P74-1-1 was significantly reduced compared to that of P74-1-0 at all ages. And at 28 d, the porosity of P74-1-1 was 1.84% lower than that of P80-1-0. This suggested that the improvement of blends and the addition of chemical admixtures could also reduce the porosity of cement mortar, thus improving its durability.

In this paper, this study found that the effective utilization of composite admixtures reduced the amount of clinker used in the limestone-cement based composite system while optimizing cement grinding efficiency and facilitating the dissolution of ferric phases to react with aluminates, ultimately enhancing the mechanical properties of cement mortar. Future research could consider the long-term study of the effect of JT-GA cement in concrete.

Acknowledgement

This research was financially supported by the China Resources Building Materials Technology Holdings Limited.

REFERENCES

[1] Mahaboob Basha S, Bhupal Reddy C, Vasugi K. Strength behaviour of geopolymer concrete replacing fine aggregates by M-sand and E-waste[J]. Int. J. Eng. Trends Technol, 2016, 40: 401-407.
[2] Skibsted J, Snellings R. Reactivity of supplementary cementitious materials (SCMs) in cement blends[J]. Cement and Concrete Research, 2019, 124: 105799.
[3] Puerta-Falla G, Kumar A, Gomez-Zamorano L, et al. The influence of filler type and surface area on the hydration rates of calcium aluminate cement[J]. Construction and Building Materials, 2015, 96: 657-665.
[4] Allahverdi A, Salem S. Simultaneous influences of microsilica and LS powder on properties of portland cement paste[J]. Ceramics-Silikaty, 2010, 54(1): 65-71.
[5] Bonavetti V, Donza H, Menendez G, et al. LS filler cement in low w/c concrete: A rational use of energy[J]. Cement and concrete research, 2003, 33(6): 865-871.
[6] Nehdi M, Mindess S, Aïtcin P C. Optimization of high strength LS filler cement mortars[J]. Cement and concrete research, 1996, 26(6): 883-893.
[7] Menéndez G, Bonavetti V, Irassar E F. Strength development of ternary blended cement with LS filler and blast-furnace slag[J]. Cement and Concrete Composites, 2003, 25(1): 61-67.
[8] Berodier E, Scrivener K. Understanding the Filler Effect on the Nucleation and Growth of C-S-H[J]. Journal of the American Ceramic Society, 2014, 97(12): 3764-3773.
[9] Machner A, Zajac M, Haha M B, et al. Portland metakaolin cement containing dolomite or LS–Similarities and differences in phase assemblage and compressive strength[J]. Construction and Building Materials, 2017, 157: 214-225.
[10] De Weerdt K, Kjellsen K O, Sellevold E, et al. Synergy between fly ash and LS powder in ternary cements[J]. Cement and concrete composites, 2011, 33(1): 30-38.
[11] Adu-Amankwah S, Zajac M, Stabler C, et al. Influence of LS on the hydration of ternary slag cements[J]. Cement and Concrete Research, 2017, 100: 96-109.
[12] Chen J, Jia J, Zhu M, et al. Advances of alkanolamine in hydration of Portland cement[J]. Materials Today Communications, 2023, 37: 107129.
[13] Wang J, Ma B, Tan H, et al. Hydration and mechanical properties of cement-marble powder system incorporating triisopropanolamine[J]. Construction and Building Materials, 2021, 266: 121068.
[14] SHI C, LIU H, LI P, et al. Effects of triisopropanolamine on hydration and microstructure of Portland LS cement[J]. Journal of the Chinese Ceramic Society, 2011, 39(10): 1673-1681.
[15] Shi Z, Shi C, Liu H, et al. Effects of triisopropanol amine, sodium chloride and LS on the compressive strength and hydration of Portland cement[J]. Construction and Building Materials, 2016, 125: 210-218.
[16] Ma S, Li W, Zhang S, et al. Study on the hydration and microstructure of Portland cement containing diethanol-isopropanolamine[J]. Cement and Concrete Research, 2015, 67: 122-130.

[17] Lu X, Ye Z, Zhang L, et al. The influence of ethanol-diisopropanolamine on the hydration and mechanical properties of Portland cement[J]. Construction and Building Materials, 2017, 135: 484-489.
[18] Assaad J J, Asseily S E, Harb J. Use of cement grinding aids to optimise clinker factor[J]. Advances in cement research, 2010, 22(1): 29-36.
[19] Xu Z, Li W, Sun J, et al. Research on cement hydration and hardening with different alkanolamines[J]. Construction and Building Materials, 2017, 141: 296-306.
[20] Katsioti M, Tsakiridis P E, Giannatos P, et al. Characterization of various cement grinding aids and their impact on grindability and cement performance[J]. Construction and Building Materials, 2009, 23(5): 1954-1959.
[21] Cheung J, Jeknavorian A, Roberts L, et al. Impact of admixtures on the hydration kinetics of Portland cement[J]. Cement and concrete research, 2011, 41(12): 1289-1309.
[22] Shi Z, Shi C, Liu H, et al. Effects of triisopropanol amine, sodium chloride and limestone on the compressive strength and hydration of Portland cement[J]. Construction and Building Materials, 2016, 125: 210-218.
[23] De Weerdt K, Haha M B, Le Saout G, et al. Hydration mechanisms of ternary Portland cements containing limestone powder and fly ash[J]. Cement and Concrete Research, 2011, 41(3): 279-291.
[24] Dilnesa B Z, Lothenbach B, Le Saout G, et al. Iron in carbonate containing AFm phases[J]. Cement and Concrete Research, 2011, 41(3): 311-323.
[25] Zou F, Tan H, He X, et al. Effect of triisopropanolamine on compressive strength and hydration of steaming-cured cement-fly ash paste[J]. Construction and Building Materials, 2018, 192: 836-845.
[26] Sandberg P J, Doncaster F. On the mechanism of strength enhancement of cement paste and mortar with triisopropanolamine[J]. Cement and concrete research, 2004, 34(6): 973-976.
[27] Shaikh F U A, Supit S W M. Mechanical and durability properties of high volume fly ash (HVFA) concrete containing calcium carbonate (CaCO3) nanoparticles[J]. Construction and building materials, 2014, 70: 309-321.
[28] Pang B, Zhou Z, Xu H. Utilization of carbonated and granulated steel slag aggregate in concrete[J]. Construction and building materials, 2015, 84: 454-467.
[29] Zhang B, Tan H, Ma B, et al. Preparation and application of fine-grinded cement in cement-based material[J]. Construction and Building Materials, 2017, 157: 34-41.
[30] Matschei T, Lothenbach B, Glasser F P. The role of calcium carbonate in cement hydration[J]. Cement and concrete research, 2007, 37(4): 551-558.